Atomistic determination of flexoelectric properties of crystalline dielectrics

R. Maranganti[1] and P. Sharma[1,2,*]
[1]*Department of Mechanical Engineering, University of Houston, Houston, Texas 77204, USA*
[2]*Department of Physics, University of Houston, Houston, Texas 77204, USA*
(Received 19 February 2009; revised manuscript received 19 July 2009; published 21 August 2009)

Upon application of a uniform strain, internal sublattice shifts within the unit cell of a *noncentrosymmetric* dielectric crystal result in the appearance of a net dipole moment: a phenomenon well known as piezoelectricity. A macroscopic *strain gradient* on the other hand can induce polarization in dielectrics of any crystal structure, even those which possess a centrosymmetric lattice. This phenomenon, called *flexoelectricity*, has both bulk and surface contributions: the strength of the bulk contribution can be characterized by means of a material property tensor called the *bulk flexoelectric tensor*. Several recent studies suggest that strain-gradient induced polarization may be responsible for a variety of interesting and anomalous electromechanical phenomena in materials including electromechanical coupling effects in nonuniformly strained nanostructures, "dead layer" effects in nanocapacitor systems, and "giant" piezoelectricity in perovskite nanostructures among others. In this work, adopting a lattice dynamics based microscopic approach we provide estimates of the flexoelectric tensor for certain cubic crystalline ionic salts, perovskite dielectrics, *III-V* and *II-VI* semiconductors. We compare our estimates with experimental/theoretical values wherever available and also revisit the validity of an existing empirical scaling relationship for the magnitude of flexoelectric coefficients in terms of material parameters. It is interesting to note that two independent groups report values of flexoelectric properties for perovskite dielectrics that are orders of magnitude apart: Cross and co-workers from Penn State have carried out experimental studies on a variety of materials including barium titanate while Catalan and co-workers from Cambridge used theoretical *ab initio* techniques as well as experimental techniques to study paraelectric strontium titanate as well as ferroelectric barium titanate and lead titanate. We find that, in the case of perovskite dielectrics, our estimates agree to an order of magnitude with the experimental and theoretical estimates for strontium titanate. For barium titanate however, while our estimates agree to an order of magnitude with existing *ab initio* calculations, there exists a large discrepancy with experimental estimates. The possible reasons for the observed deviations are discussed.

DOI: 10.1103/PhysRevB.80.054109 PACS number(s): 77.65.−j

I. INTRODUCTION

In a continuum framework, the *linear* polarization response **P** to a strain field ε in a crystalline dielectric is typically given as

$$P_i = e_{ijk}\varepsilon_{jk} \tag{1}$$

e is the third-rank piezoelectric tensor which couples strain to polarization. **e**, being an odd order tensor, vanishes identically for centrosymmetric crystals and thus only those dielectrics which possess a noncentrosymmetric crystal structure exhibit piezoelectricity.

In crystalline centrosymmetric dielectrics, where piezoelectricity is absent (**e**=0), a nonuniform strain can locally break the inversion symmetry of the unit cell, resulting in an induced dipole moment. In such a case, the bulk contribution to the polarization as a response to an applied macroscopic strain gradient may be written as

$$P_i = \mu_{ijkl}u_{j,kl}. \tag{2}$$

Here **u** is the displacement and the commas indicate differentiation with respect to the respective spatial coordinates. The phenomenological fourth-order tensor $\boldsymbol{\mu}$ introduced in Eq. (2) is known as the flexoelectric tensor and the associated phenomenon wherein a macroscopic strain gradient induces a linear polarization response in a dielectric is termed *flexoelectricity*.[1] A macroscopic strain gradient implies that the gradient in strain exists over a macroscopically large length scale $L \gg a$ (where a is the characteristic length scale of the material). In crystals a can be taken to be the lattice parameter.$\boldsymbol{\mu}$, being a tensor of even order, is nonzero for crystals of any symmetry. Therefore the polarization response to an applied deformation in a dielectric may be rewritten as

$$P_i = e_{ijk}\varepsilon_{jk} + \mu_{ijkl}u_{j,kl}. \tag{3}$$

The phenomenon of flexoelectricity in crystalline dielectrics was first predicted by Maskevich and Tolpygo;[2] a phenomenological description was later proposed by Kogan[3] who included a term coupling the polarization and the strain gradient in the thermodynamic potential of the form

$$f_{ijkl}P_i u_{j,kl}. \tag{4}$$

More recently, Tagantsev[4,5] has investigated this phenomenon in detail and has clarified several issues regarding the bulk nature of flexoelectricity and contributions due to surface and dynamic effects. The fourth-order tensor **f** introduced in Eq. (4) can be related to the flexoelectric tensor $\boldsymbol{\mu}$ in Eq. (3) and it symmetries are now well known. Kogan[3] estimated the flexoelectric constants μ_{ijkl} to be of the order of e/a, where e is the electronic charge and a, the lattice parameter. Multiplication by the dielectric constant was later suggested which appears to have been confirmed experimentally in a series of studies by Cross and co-workers.[6–9]

Yet another body of work, which parallels the theory of flexoelectricity in some ways, is the polarization-gradient theory due to Mindlin.[10] Based on the long-wavelength limit of the shell model of lattice dynamics, Mindlin[10] found that the core shell and the shell-shell interactions could be incorporated phenomenologically by including the coupling of polarization gradients to strain and the coupling of polarization gradients to polarization gradients, respectively, in the thermodynamic potential [Eqs. (5a) and (5b)]

$$d_{ijkl}P_{i,j}\varepsilon_{kl} \tag{5a}$$

$$b_{ijkl}P_{i,j}P_{k,l}. \tag{5b}$$

Material property tensors **d** and **b** are constants introduced by Mindlin in this polarization-gradient theory. The polarization-gradient strain coupling (represented by tensor **d**) and the polarization strain-gradient coupling (represented by tensor **f**) is often included in the energy density expression as a Lifshitz invariant[11,12] as shown in Eq. (6) on account of the fact that total derivatives cannot occur in the expression for energy.

$$h_{ijkl}(u_{ij}P_{k,l} - P_k u_{ij,l}) \tag{6}$$

h is yet another material property tensor and is given by a combination of tensors **d** and **f**. The symmetries of the tensors **d** and **b** are known.[10] Under the framework of Mindlin's polarization-gradient theory, Askar *et al.*[13] arrived at theoretical estimates of tensors **d** and **b** by relating them to shell-model parameters for the cases of NaCl, NaI, KI, and KCl.

It can be seen that the dispersive contributions due to the terms in Eqs. (4) and (5a) are of the same order in the wave vector **k**. Askar *et al.*[13] used a lattice-dynamical method to theoretically estimate the numerical values of the material property tensor **d** which occurs in Mindlin's polarization-gradient theory (which does not include flexoelectric terms) for certain cubic crystalline materials. However, since the dispersive contributions due to the polarization-gradient terms of the form of Eq. (5a) and the flexoelectric terms of the form of Eq. (4) are of the same order in the wave vector **k**, the values estimated in Ref. 13 are more likely a combination of components of tensor **d** and those of the tensor **f**.

In addition to the arguments presented above, yet another motivation to include higher-order gradients of strain and polarization in the formulation of a continuum theory for crystalline dielectrics appears while investigating dynamic phenomena. Classical electromagnetism may be safely applied to excitations belonging to any part of the spectrum whereas *classical* linear elasticity (wherein the elastic energy involves only the first derivatives of displacement) is a "long-wavelength theory" and designed to be applicable only in a certain frequency regime. Therefore a hybrid electromechanical theory is limited in its applicability due to its elastic part. The inclusion of gradients of strain and polarization along with higher-order inertia terms to the elastic part of the free energy can extend the applicability of a hybrid electromechanical field theory to frequencies in the region of 1 THz (far-infrared region) where dispersive effects become significant.[14,15] It should be noted that while the flexoelectric effect introduces spatial dispersion, polarization gradients (and polarization-inertia effects) can model frequency dispersion effects.

The phenomenon of flexoelectricity in crystalline dielectrics has been experimentally observed in a variety of contexts: bending of crystal plates[16] and measurements of thin films.[17] We note that the term flexoelectricity originated in the liquid crystal and biological membrane literature to describe curvature induced polarization in *flexed* membranes of orientable molecules. In this work however, we concern ourselves with flexoelectricity in crystalline dielectrics only. It has also been variously invoked to explain the anomalous capacitance of thin dielectric films[17] and the weak size-dependent piezoelectric behavior of carbon and boron-nitride nanotubes.[18,19] Macroscopic electromechanical effects in dislocated diatomic crystals of nonpiezoelectric dielectrics, wherein large strain gradients in the vicinities of dislocations lead to induced polarization,[20] may also be explained using flexoelectricity. Some works have reported large flexoelectric effects in low dimensional systems such as nanographitic systems[21] and two-dimensional (2D) boron-nitride sheets.[22] In addition, some recent theoretical works seem to suggest that flexoelectric effects can assume importance in various nanoscale electromechanical phenomena, especially in high-dielectric materials e.g., "giant" piezoelectricity in perovskite dielectric nanostructures, piezoelectric composites without using piezoelectric materials among others.[23–26] However, very few atomistic investigations to estimate the flexoelectric constants exist in the literature. Experimental determination of flexoelectric constants for some perovskite dielectrics have been carried out by Cross and co-workers[6–9] and Zubko *et al.*[27] while from a theoretical viewpoint, Sahin and Dost[28] provided some estimates for $KTaO_3$ predicated on phonon-dispersion data. In the present work, using an approach outlined by Tagantsev,[4,5] we employ a lattice dynamics based method to extract the flexoelectric coefficients for certain representative ionic salts NaCl and KCl, *III-IV* semiconductors GaAs and GaP, *II-VI* semiconductors ZnO and ZnS, and finally high-dielectric constant perovskites $BaTiO_3$(BTO), $SrTiO_3$(STO) and $PbTiO_3$(PTO) in their cubic phases. We report estimates for the flexoelectric constants from both density-functional theory (DFT) based *ab initio* lattice dynamics and empirical shell models. Wherever possible, we compare our results with previously published theoretical calculations or experimental results. Flexoelectric coefficients of perovskite dielectric materials are of particular interest—large flexoelectric effects have been consistently observed in experimental studies on bent thin films of high-permittivity perovskite dielectric materials[6–9] as well as atomistic simulations on bent nanostructures.[21,22] This has important ramifications in perovskite dielectric thin-film/nanostructure-based technologies such as nanocapacitors and energy harvesting applications.[23–25,29]

The outline of our paper is as follows. In Sec. II, we present a brief overview of a continuum theory involving the first gradients of strain and polarization. We show how inclusion of appropriate terms in the electroelastic energy density can lead to a linear polarization response to an applied strain gradient i.e., flexoelectricity. In Sec. III, a microscopic lattice dynamics based analysis is carried out which identifies the atomistic origins of flexoelectricity. Certain subtleties associ-

ated with this phenomenon are also discussed. Section IV outlines a recipe[4,5] to calculate bulk flexoelectric constants for crystalline dielectrics from lattice-dynamical data. In Sec. V, we bring out some differences between the approach of Tagantsev to calculate flexoelectric constants and that of Askar *et al.*'s[13] to calculate Mindlin's polarization-gradient constants. The numerical values of the flexoelectric constants for some selected materials presented in Sec. VI. Finally we discuss the physical reasons responsible for the high flexoelectric constants displayed by perovskite dielectric materials in Sec. VII as well as the reasons for the observed discrepancies between our theoretical estimates the available limited experimental data.

II. CONTINUUM FLEXOELECTRICITY: LINEAR POLARIZATION RESPONSE DUE TO A STRAIN GRADIENT

The general formulation of an electromechanical theory involving first gradients of strain and polarization has been discussed elsewhere.[28] Here we provide a brief summary. If one includes terms involving gradients of strain and polarization in the thermodynamic potential, then a hybrid internal energy density function can be written of the form

$$\Sigma = \frac{1}{2}a_{kl}P_kP_l + h_{ijk}P_iP_{j,k} + e_{ijk}P_i\varepsilon_{jk} + \frac{1}{2}b_{ijkl}P_{i,j}P_{k,l} + \frac{1}{2}c_{ijkl}\varepsilon_{ij}\varepsilon_{kl}\cdots + d_{ijkl}P_{i,j}\varepsilon_{kl} + f_{ijkl}P_iu_{j,kl} + r_{ijklm}\varepsilon_{ij}u_{k,lm} + g_{ijklmn}u_{i,jk}u_{l,mn}\cdots \quad (7)$$

a, **e**, and **c** are the familiar second-order reciprocal dielectric susceptibility tensor, third order piezoelectric tensor and the fourth-order elastic constant tensor respectively. **f** is the fourth-order flexoelectric tensor introduced in Eq. (4) while **b** and **d** are fourth-order tensors from Eq. (5). The third-order tensor **h** couples the polarization to its gradient while the fifth order tensor **r** couples strain and strain gradient. Tensor **r** is sometimes referred to as the acoustic gyroscopic tensor. Tensor **g** represents elastic nonlocality and dictates the strength of the biquadratic strain-gradient coupling:[14,15] it also serves the purpose of smoothing out distribution of fields.

Balance equations and constitutive relations for the electromechanical stresses can be derived by carrying out a variational analysis of the Lagrangian derivable from Eq. (7). The interested reader is referred to the paper by Sahin and Dost[28] wherein this variational analysis has been carried out in exhaustive detail.

In the absence of an external electric field and free charges, the following expression involving the polarization and its gradient can be deduced from the balance equations and constitutive laws

$$(a_{ij} + \varepsilon_0^{-1}\delta_{ij})P_j = d_{ijkl}\varepsilon_{kl,j} - (e_{ijk}\varepsilon_{jk} + f_{ijkl}u_{j,kl}) + h_{ijk}(P_{k,j} - P_{j,k}) + b_{ijkl}P_{k,lj}. \quad (8)$$

For a centrosymmetric material, the third order tensors in Eq. (8) vanish

$$(a_{ij} + \varepsilon_0^{-1}\delta_{ij})P_j = d_{ijkl}\varepsilon_{kl,j} - f_{ijkl}u_{j,kl} + b_{ijkl}P_{k,lj}. \quad (9)$$

The above expression shows that following the energy density expression of Eq. (7), the polarization response is linearly related to the strain gradient.

From a microscopic point of view, the terms involving polarization gradients in the expression for the internal energy density in Eq. (7) can be shown to bear analogs to certain interaction energy terms occurring in a shell-type lattice-dynamical model. In particular, the shell-shell interactions can be modeled through the biquadratic coupling of polarization gradients to themselves while the core-shell interactions can be modeled via the coupling of polarization gradients to strain. Using this approach, Askar *et al.*[13] carried out explicit calculations to estimate the independent components of the tensors **b** and **d** for NaCl and KCl in terms of corresponding shell-model parameters. On the other hand, as discussed in references,[4,5] a simple rigid-ion model, which approximates atoms as consisting of ionic cores devoid of a shell of electrons, suffices to make the connection with the phenomenological flexoelectric coupling. In the following section, we will outline Tagantsev's approach to calculating the flexoelectric constants using a simple rigid-ion model for lattice dynamics. Further, we will also bring out some important differences between Tagantsev's approach to capture flexoelectricity induced spatial dispersion using a rigid-ion model and Askar *et al.*'s[13] approach to capture polarization-gradient induced frequency dispersion using a shell-type lattice-dynamical model. In doing so, we also hope to make physically transparent, the microscopic origins of both flexoelectricity and polarization-gradient effects.

III. POLARIZATION DUE TO A UNIFORM STRAIN GRADIENT: MICROSCOPIC ANALYSIS

In the following, parts of this section and the next summarizes Tagantsev's work[4] to aid the reader. Consider a *uniform* strain gradient in a macroscopically large (but finite) crystal

$$\varepsilon_{ij}(\mathbf{x}) = \varepsilon_{ij}(0) + \frac{\partial \varepsilon_{ij}}{\partial x_k}x_k. \quad (10)$$

Integrating both sides of Eq. (10)

$$\int \varepsilon_{ij}(\mathbf{x})d^3x = \int \varepsilon_{ij}(0)d^3x + \int \frac{\partial \varepsilon_{ij}}{\partial x_k}x_kd^3x. \quad (11)$$

If the gradient is uniform, then $\frac{\partial \varepsilon_{ij}}{\partial x_k}$ is constant and $\int x_k d^3x = 0$ (if one assumes that the crystalline structure under consideration is centered at the origin). Therefore,

$$\varepsilon_{ij}(0) = V^{-1}\int \varepsilon_{ij}(\mathbf{x})d^3x. \quad (12)$$

Here x_k are the Cartesian coordinates of a point inside the undeformed crystal.

In the presence of a strain given by Eq. (12), a particle initially at **R** is shifted to position **R′**

$$\mathbf{R}' = \mathbf{R} + \mathbf{r}. \quad (13)$$

Here **r** is

$$r_i = \varepsilon_{ij}(0)R_j + \frac{1}{2}\frac{\partial \varepsilon_{ij}}{\partial x_k}R_jR_k + u_i^{(1)}(\mathbf{R}) + u_i^{(2)}(\mathbf{R}), \quad (14)$$

$\mathbf{u}^{(1)}(\mathbf{R})$ and $\mathbf{u}^{(2)}(\mathbf{R})$ are the linear response of the internal strain to the macroscopic strain ε_{ij} and its gradient $\frac{\partial \varepsilon_{ij}}{\partial x_k}$. Following the assumption of linearity, $\mathbf{u}^{(1)}$ and $\mathbf{u}^{(2)}$ can be cast in the form

$$u_i^{(1)}(\mathbf{R}) = u_{i,p}^{(1)} = A_{i,p}^{jk}\varepsilon_{jk}(\mathbf{R}); \quad u_i^{(2)}(\mathbf{R}) = u_{i,p}^{(2)} = B_{i,p}^{jkl}\frac{\partial \varepsilon_{jk}}{\partial x_l}(\mathbf{R}). \quad (15)$$

$\mathbf{u}_p^{(1)}$ denotes the sublattice shift of the p^{th} atom in the unit cell under the influence of a uniform strain; this quantity vanishes for all atoms in a centrosymmetric unit cell. On the other hand, $\mathbf{u}_p^{(2)}$ signifies the internal displacement of the p^{th} atom in response to the applied strain gradient and is nonzero in principle for crystals of any symmetry.

Following the displacements of Eq. (15), the polarization change due to such internal motions is given by

$$\delta\mathbf{P} = (V')^{-1}\sum_{\mathbf{R}'} Q(\mathbf{R}')\mathbf{R}' - (V)^{-1}\sum_{\mathbf{R}} Q(\mathbf{R})\mathbf{R}. \quad (16)$$

V and V' are the volumes of the crystal before and after deformation and $Q(\mathbf{R})$ $Q(\mathbf{R})$ is the charge of the particle at $\mathbf{R}$. From Eqs. (15) and (16),

$$\delta P_i = \underbrace{\varepsilon_{ij}(0)P_j^0 - \varepsilon_{jj}(0)P_i^0}_{\text{Spontaneous Polarization Contribution}} + \underbrace{(V)^{-1}\sum_{\mathbf{R}} Q(\mathbf{R})u_i^{(1)}(\mathbf{R})}_{\text{Piezoelectric Contribution}} + \underbrace{\frac{1}{6}Q_{jk}\frac{\partial \varepsilon_{ij}}{\partial x_k}}_{\text{Quadrupole moment contribution}} + \underbrace{\frac{I}{2}\frac{\partial \varepsilon_{ij}}{\partial x_j} + (V)^{-1}\sum_{\mathbf{R}} Q(\mathbf{R})u_i^{(2)}(\mathbf{R})}_{\text{Flexoelectric Contribution}}. \quad (17)$$

In Eq. (17), $\mathbf{P}^0$ is the spontaneous polarization of the crystal in the undeformed configuration and $Q_{ij}\mathbf{Q}$ is the average quadrupole moment density. $\mathbf{P}^0$, $Q_{ij}\mathbf{Q}$, and I are defined as

$$\mathbf{P}^0 = (V)^{-1}\sum_{\mathbf{R}} Q(\mathbf{R})(\mathbf{R}), \quad (18a)$$

$$Q_{ij} = (V)^{-1}\sum_{\mathbf{R}} Q(\mathbf{R})(3R_iR_j - \delta_{ij}R^2), \quad (18b)$$

$$I = (V)^{-1}\sum_{\mathbf{R}} Q(\mathbf{R})R^2. \quad (18c)$$

As argued in Ref. 4, to estimate the flexoelectric response under an applied strain gradient, the polarization induced should be measured under the conditions of zero macroscopic electric field ensuring the elimination of spurious spontaneous polarization and surface polarization effects. The macroscopic electric field is associated with the nonanalyticity of the lattice-dynamical matrix at near zero wave vectors. Therefore, while investigating flexoelectric coefficients using lattice-dynamical methods, the nonanalytical contribution to the dynamical matrix should be removed. This point will be further elaborated in Sec. III. Under such conditions, the spontaneous polarization $\mathbf{P}^0$ and the quadrupole moment density $Q_{ij}\mathbf{Q}$ both vanish. Further, the induced polarization caused due to internal displacement of atoms $u_i^{(1)}(\mathbf{R})$ in response to a macroscopic strain corresponds to the piezoelectric effect. Thus, the induced polarization due to flexoelectricity can be isolated as

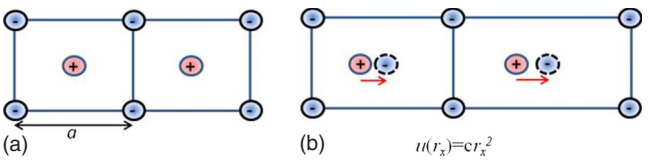

FIG. 1. (Color online) (a) Shows the undeformed stress-free configuration of a portion of a 2D diatomic ionic solid. (b) shows the deformed configuration wherein each atom is subjected to an inhomogeneous displacement of the form $u(r_x)=cr_x^2$, where r_x is the x coordinate of the position vector of that atom.

$$P_{fl,i} = \frac{I}{2}\frac{\partial \varepsilon_{ij}}{\partial x_j} + v^{-1}Q_pB_{i,p}^{jkl}\frac{\partial \varepsilon_{jk}}{\partial x_l}. \quad (19)$$

v is the volume of the unit cell while Q_pQ_p is the *effective* charge of the p^{th} atom. The first term on the right-hand side of Eq. (19) can be identified as the surface flexoelectric contribution[1,2] while the second term can be identified as the bulk flexoelectric contribution.

Thus the bulk flexoelectric tensor μ_{ijkl} can be identified from Eq. (19) as

$$\mu_{ijkl} = v^{-1}Q_pB_{i,p}^{jkl}. \quad (20)$$

For materials with cubic symmetry $Fm\bar{3}m$ or $Pm3m$, the bulk flexoelectric tensor μ has the following decomposition:[1]

$$\mu_{ijkl} = (\mu_{11} - \mu_{12} - 2\mu_{44})\delta_{ijkl} + \mu_{12}\delta_{ij}\delta_{kl} + \mu_{12}(\delta_{ik}\delta_{jl} + \delta_{il}\delta_{jk}). \quad (21)$$

Here, δ_{ijkl} is 1 for all indices equal and zero otherwise. It may be noted from Eq. (19) that polarization due to flexoelectricity is induced as a consequence of internal shifts among atoms within a unit cell due to an applied strain gradient; i.e., a dipole is created within a unit cell when atoms carrying opposite charges suffer a net displacement with respect to each other leading to a macroscopic polarization. Therefore, for flexoelectricity to exist, it is imperative that a strain gradient exists at the level of a unit cell; i.e., there is a spatial variation of strain within the unit cell.

Yet another subtlety relates to the distinction between surface and bulk flexoelectricity. The phenomenon of flexoelectricity is pictorially explained as follows. Consider again an arrangement of atoms which form a part of periodic 2D ionic crystalline solid as shown in Fig.1(a). For convenience, we only depict two unit cells.

In the equilibrium stress-free configuration of Fig. 1(a), the centers of positive and negative charges coincide and there is no net dipole moment. Now if an inhomogeneous displacement of the form $u(r_x)=cr_x^2$, where r_x stands for the x coordinate of an atom and c is a constant, is applied to the

stress-free configuration of Fig. 1(a) and the atoms are clamped, then dipoles are created in each unit cell as is shown in Fig. 1(b). However, this induced polarization is a result of surface flexoelectricity and corresponds to the first term on the right-hand side of Eq. (19). If, under the conditions of an inhomogeneous stress, the atoms are "unclamped" and allowed to relax, they undergo further internal shifts corresponding to the displacements $\mathbf{u}_p^{(2)}$ of Eq. (15). It is the additional polarization created due to these internal shifts which corresponds to the bulk flexoelectric effect corresponding to the second term on the right-hand side of Eq. (19).

Another point deserves mention. Even though, flexoelectricity in principle can be observed in all materials, one can see from the discussion above that in materials where effective charges of atoms Q_p are zero, say for example a single element material like graphene where no effective charges can be assigned to atoms in the unit cell, the bulk flexoelectric constant of Eq. (20) becomes zero. However, flexoelectricity can still occur in such materials purely due to electronic wave-function overlap effects. Indeed, Dumitrica *et al.*[18] demonstrated the presence of flexoelectricity induced polarization in curved carbon nanoshells. The rigid-ion model can however not take into account such effects and this is indeed a limitation of the approach we adopt in this paper. In the following section we will outline an approach to calculate $B_{i,p}^{jkl}\mathbf{B}$ [Eq. (15)] and subsequently the flexoelectric constant [Eq. (20)] from harmonic lattice dynamics.

IV. DETERMINATION OF FLEXOELECTRIC CONSTANTS: A LATTICE DYNAMICS APPROACH

Consider an acoustic wave traveling in an effectively infinite crystal with wave vector $\mathbf{k}$ such that $|\mathbf{k}|^{-1}$ is much less than the crystal dimensions but much larger than the lattice parameter a. The displacement of the p^{th} atom in the n^{th} unit cell associated with such a wave can be written as

$$r_{i,p}^n = u_{i,p} e^{i(\mathbf{k}.\mathbf{R}_p^n - \omega t)}. \tag{22}$$

The amplitude of displacement $\mathbf{u}_p$ corresponding to the p^{th} atom of a unit cell corrected to include first-order spatial and frequency dispersion effects can be written from Eq. (14) as

$$u_{i,p} = w_i + iA_{i,p}^{jk} w_j k_k - B_{i,p}^{jkl} w_j k_k k_l - G_{i,p}^j w_j \omega^2. \tag{23}$$

In Eq. (23), $\mathbf{w}$ is the amplitude of the *pure* acoustic wave. For a pure acoustic phonon mode ($\mathbf{k} -> 0$), the amplitude of displacement $u_{i,p}$ is independent of p i.e., all atoms oscillate with the same amplitude of vibration. Physically speaking, this corresponds to a uniform deformation in classical continuum elasticity. The remaining terms on the right-hand side of Eq. (23) correspond to internal shifts which occur because of the inherent discreteness of the crystal. The operator $\mathbf{G}$ corresponds to frequency dispersion corrections to the displacement amplitude and can be shown to be related to polarization-inertia effects.

Now consider the Hamiltonian of a crystal written in the harmonic approximation

$$H = \Phi_0 + \frac{1}{2}\sum_{nip} m_p (r_{i,p}^n)^2 + \frac{1}{2}\sum_{\substack{nip \\ n'i'p'}} \Phi_{ip,i'p'}^{nn'} r_{i,p}^n r_{i',p'}^{n'}. \tag{24}$$

Here, Φ_0 is the static (equilibrium) potential energy of the crystal and $\Phi_{ip,i'p'}^{nn'}$ constitute the elements of the so-called force-constant matrix. In particular,

$$\Phi_{ip,i'p'}^{nn'} = \left.\frac{\partial^2 \Phi}{\partial r_{i,p}^n \, \partial r_{i',p'}^{n'}}\right)_0 \tag{25}$$

Here, Φ is the total potential energy of the crystal assumed to be some function of the instantaneous positions of all the atoms.

Now the equations of motion for the lattice can be derived as

$$m_p \ddot{r}_{i,p}^n = -\frac{\partial \Phi}{\partial r_{i,p}^n} = -\sum_{n'i'p'} \Phi_{ip,i'p'}^{nn'} r_{i',p'}^{n'}. \tag{26}$$

The equations of motion [Eq. (26)] form an infinite set of simultaneous linear differential equations. Their solution can be simplified by exploiting the periodicity of the lattice if we choose as a solution to Eq. (27) a function of the form

$$r_{i,p}^n = u_{i,p} e^{i(\mathbf{k}.\mathbf{R}_p^n - \omega t)}. \tag{27}$$

After substituting the expression for $\mathbf{r}$ from Eq. (27) into Eq. (26), one can arrive at

$$\omega_j^2(k) u_{i,p}(\mathbf{k}j) = \sum_{i'p'} C_{ip,i'p'}(\mathbf{k}) u_{i',p'}(\mathbf{k}j). \tag{28}$$

$\mathbf{C}$ is related to the dynamical matrix and can be written in terms of the force constants as

$$C_{ip,i'p'}(\mathbf{k}) = \sum_{n'} \Phi_{ip,i'p'}^{nn'} e^{[-i\mathbf{k}.(\mathbf{R}_p^n - \mathbf{R}_{p'}^{n'})]}. \tag{29}$$

The set of equations given by Eq. (28) can be solved in a perturbative manner for small $\mathbf{k}$ by the method of long waves. We will accordingly expand all the quantities appearing in Eq. (28) in powers of $\mathbf{k}$ up to second order.

$$C_{ip,i'p'}(\mathbf{k}) = C_{ip,i'p'}^{(0)} + \sum_j C_{ip,i'p'}^{(1)j} k_j + \frac{1}{2}\sum_{\gamma\lambda} C_{ip,i'p'}^{(2)jl} k_j k_l + \cdots \tag{30a}$$

$$u_{i,p}(\mathbf{k}j) = u_{i,p}^{(0)}(\mathbf{k}j) + u_{i,p}^{(1)}(\mathbf{k}j) + u_{i,p}^{(2)}(\mathbf{k}j) + \cdots \tag{30b}$$

$$\omega_j(\mathbf{k}) = \omega_j^{(1)}(\mathbf{k}) + \omega_j^{(2)}(\mathbf{k}) + \cdots \tag{30c}$$

In case of ionic materials, the perturbative expansion of Eqs. (30a)–(30c) presents problems because even the lowest-order term in the expansion of the dynamical matrix diverges because of long-range electrostatic forces. This is dealt with by separating the electrostatic field at a point into a local Lorentzian field plus a global macroscopic electric field. Further, the contribution of the macroscopic field to the dynami-

cal matrix can be identified with the nonanalytical terms of the dynamical matrix which cause divergent behavior at near zero wave vectors. The short-range contributions to the dynamical matrix due to short-range forces and the Lorentz field can then be treated in a perturbative manner. However, as has been previously pointed out, the flexoelectric coefficients, by definition, measure the polarization response under the application of a uniform strain gradient in the absence of a macroscopic electric field. Thus in case of both weakly polar materials (such as GaAs) and highly polar materials (such as BTO), we exclude the contribution of the macroscopic electric field while calculating the dynamical matrix in Eq. (30). This contribution is likely to be small for less polar materials such as GaAs while one expects a large contribution due to the macroscopic field in a highly polar solid such as BTO.

The expansion coefficients in Eq. (30a) are given by

$$C^{(0)}_{ip,i'p'} = \sum_{n'} \Phi^{nn'}_{ip,i'p'} \tag{31a}$$

$$C^{(1)j}_{ip,i'p'} = \sum_{n'} \Phi^{nn'}_{ip,i'p'} (\mathbf{R}^n_p - \mathbf{R}^{n'}_{p'})_j \tag{31b}$$

$$C^{(2)jl}_{ip,i'p'}(k,k') = -\sum_{n'} \Phi^{nn'}_{ip,i'p'} (\mathbf{R}^n_p - R^{n'}_{p'})_j (R^n_p - R^{n'}_{p'})_l. \tag{31c}$$

As discussed before, the force constants occurring in Eqs. (31a)–(31c) are such that the macroscopic field contribution has been excluded.

On substituting Eqs. (31a)–(31c) in Eq. (28), we have

$$C^{(0)}_{ip,i'p'} u^{(0)}_{i'p'} = 0, \tag{32a}$$

$$C^{(0)}_{ip,i'p'} u^{(1)}_{i'p'} = -ik_j C^{(1)j}_{ip,i'p'} u^{(0)}_{i'p'}, \tag{32b}$$

$$C^{(0)}_{ip,i'p'} u^{(2)}_{i'p'} = -ik_j C^{(1)j}_{ip,i'p'} u^{(1)}_{i'p'} - \frac{k_j k_l}{2} C^{(2)jl}_{ip,i'p'} u^{(0)}_{i'p'} + \omega^2 m_p u^{(0)}_{ip}. \tag{32c}$$

One can solve for $u^{(0)}_{ip}$, $u^{(1)}_{ip}$ and $u^{(2)}_{ip}$ to obtain

$$\mathbf{u}^{(0)}_p = \mathbf{w}, \tag{33a}$$

$$u^{(1)}_{ip} = -\sum_{p''} \Gamma_{ip,i'p'} C^{(1)j}_{ip,i''p''} ik_j w_{i''}, \tag{33b}$$

$$u^{(2)}_{ip} = \sum_{p''} \Gamma_{ip,i''p''} (\omega^2 \mu_{p'} \delta_{pp''} \delta_{i'i''} - k_j k_l \tilde{T}^{jl}_{i'p',i''p''}) w_{i''}. \tag{33c}$$

In Eqs. (33a)–(33c), $\mathbf{w}$ is any arbitrary vector in space. The matrix $\mathbf{\Gamma}$ in Eqs. (33b) and (33c) is the *inverse* of the singular matrix defined in a special way. For a unit cell containing r atoms, p varying from 0 to $r-1$, the $3r \times 3r$ matrix $\mathbf{\Gamma}$ in Eqs. (33b) and (33c) is defined as

$$\Gamma_{ip,i'p'} = \Gamma^{(3r-3)}_{ip,i'p'} \quad p,p' \neq 0 = 0 \quad \text{otherwise}. \tag{34}$$

Here, $\mathbf{\Gamma}^{(3r-3)}$ is the inverse to the $(3r-3)\times(3r-3)$ matrix $C^{(0)}_{ip,i'p'}$ $(p,p' = 1,2,\ldots,r-1)$.

Further, the following definitions hold for the matrix $\tilde{\mathbf{T}}$ introduced in Eq. (33c):

$$\tilde{T}^{jl}_{ip,i'p'} = T^{jl}_{ip,i'p'} - \frac{\delta_{pp'}}{s} \sum_{p'',p'''} T^{jl}_{ip'',i'p'''}, \tag{35a}$$

$$T^{jl}_{ip,i'p'} = C^{(1)j}_{ip,i''p''} \Gamma_{i''p'',i'''p'''} C^{(1)l}_{i'''p''',i'p'} + \frac{1}{2} C^{(2)jl}_{ip,i'p'}. \tag{35b}$$

From Eqs. (23) and (33a)–(33c), we can conclude that

$$A^{lj}_{i,p} = -\sum_{p''} \Gamma_{ip,i'p'} C^{(1)j}_{i'p',lp''},$$

$$B^{jkl}_{i,p} = \sum_{p''} \Gamma_{ip,i'p'} \tilde{T}^{kl}_{i'p',jp''},$$

$$G^j_{i,p} = -\Gamma_{ip,jp'} \mu_{p'}.$$

Thus we arrive at expressions for **A**, **B**, and **G** in terms of matrices, which can be related to the real-space interatomic force constants.

One can in principle generate the phonon dispersion over a sufficiently large grid of wave vectors by *ab initio* or empirical lattice dynamics and then do an inverse Fourier transform in order to generate the interatomic force constants $\Phi^{nn'}_{ip,i'p'}$ up to a given number of neighbors corresponding to a rigid-ion lattice-dynamical model. The denser the grid of phonon wave vectors, the larger is the distance of the farthest neighbor to an atom for which interatomic constants can be calculated. Therefore, for a material like BTO for which long-range interatomic forces become important, one would be better served by generating the phonon dispersions over a large grid of wave vectors.

V. TAGANTSEV'S APPROACH TO ESTIMATE FLEXOELECTRIC CONSTANTS VS ASKAR *et al.*'S APPROACH TO CALCULATE POLARIZATION-GRADIENT CONSTANT

Tagantsev's[4] approach to calculating flexoelectric constants employs a simple rigid-ion model. The flexoelectric polarization in this approach stems from the fact that in the long-wavelength limit, different atoms (which correspond to ionic cores) in the same unit cell move by different amounts which corresponds to first-order dispersive corrections. If one revisits the expression for the amplitude of displacement of the p^{th} atom in a unit cell in the long-wavelength limit, one notices that the dispersive correction term involving **A** corresponds to the internal displacement of the atom in response to a uniform strain $\mathbf{u}^{(1)}_p$, while the terms involving **B** and **G** correspond to the internal displacement of the atom in response to an applied strain gradient $\mathbf{u}^{(2)}_p$.

The flexoelectric polarization simply spawns from the dipole created within a unit cell due to internal displacements of various ionic cores within the unit cell,

$$P_{flexo,i} = v^{-1} Q_p u_{i,p}^{(2)}. \tag{37}$$

On the other hand, Askar *et al.*[13] uses a shell-type model to extract the polarization-gradient constants **b** and **d** for centrosymmetric crystals NaCl, NaI, KCl, and KI. In order to illustrate their approach, consider a NaCl-like crystal with two atoms per unit cell. In a shell-like model, the outermost electron shell is considered to be a rigid spherical "shell," which can move with respect to the massive ionic "core" which consists of the nucleus and the inner electron shells. The position of p^{th} atom in the n^{th} unit cell is denoted by $\mathbf{r}_p^n$.

The charge of the p^{th} atom is given by

$$Q_p = X_p + Y_p, \tag{38}$$

where X_p and Y_p are the charges of the core and shell of the p^{th} atom respectively. The constraint of neutrality implies

$$\sum_p Q_p = 0. \tag{39}$$

For the shell model, the positions of both the core and the shell, before deformation are given by $\mathbf{r}_p^n$. Their positions after deformation are, respectively,

$$\mathbf{R}_p^{n,1} = \mathbf{r}_p^n + \mathbf{u}_p^n,$$

$$\mathbf{R}_p^{n,2} = \mathbf{r}_p^n + \mathbf{u}_p^n + \mathbf{w}_p^n. \tag{40}$$

u is the displacement of the core and **w** is the displacement of the shell with respect to the core.

The fact that the core and shell of each ion/atom carry different charges and that they can be displaced with respect to each other implies that when an effective electric field acts on the core and on the shell, they will suffer a relative displacement inducing a dipole moment at the ion/atom location proportional to the electric-field strength. The proportionality constant is given by the polarizability of the ion α_p which enters into the shell model as a parameter. At the same time, even in the absence of an effective field, when two ion cores are brought closer together, the equilibrium positions of the centers of the corresponding shells need not coincide with the position of the cores, so that a dipole moment is induced on each ion/atom which is proportional to the displacement of the core. Thus the deformability and polarizability of each ion is included in the shell model. While in the rigid-ion model, the dipole moment induced due to an electric field is only due to movement of rigid ions, in case of a shell model, additional contributions to the dipole moment arise as a result of the polarizability of the ion and also as a contribution due to the redistribution of charge in the region of overlap between neighboring ions. This latter contribution exists even in the absence of the first and is present for materials such as graphene and silicon which are made up of atoms and not ions. This is perhaps one of the biggest disadvantages of using a rigid-ion model.

Now, under the assumption of a rigid-ion model, let us consider an acoustic wave in the crystal such that

$$\mathbf{u}_p^n = \mathbf{u}_p e^{i(\mathbf{k}.\mathbf{r}_p^n - \omega t)}; \quad \mathbf{w}_p^n = \mathbf{w}_p e^{i(\mathbf{k}.\mathbf{r}_p^n - \omega t)}. \tag{41}$$

In the long-wavelength limit, Askar *et al.*,[13] assumed that the amplitude of displacement of the cores is the same, i.e., $\mathbf{u}_p$ does not depend on p. They neglect any internal displacements among the atoms as a result of first-order dispersive effects at low k wave vectors. Instead, they assume a one-ion polarizable model wherein only one shell corresponding to a highly polarizable atom is capable of displacing with respect to its core. Say for example, in the case of NaCl, Na being numbered 1 and Cl being numbered 2, Askar *et al.*[13] approximated $\mathbf{w}_1 = 0$ owing to the low polarizability of Na compared to that of Cl. Thus, in the long-wavelength limit one has

$$\mathbf{u}_1 = \mathbf{u}_2 = \mathbf{u}$$

$$\mathbf{w}_1 = 0; \quad \mathbf{w}_2 = \mathbf{w}. \tag{42}$$

The dipole moment per unit cell (i.e., the polarization is),

$$\mathbf{P} = \frac{1}{v}[Q_1 \mathbf{u} e^{i\mathbf{k}.\mathbf{r}_1} + (Q_2 \mathbf{u} + Y_2 \mathbf{w}) e^{i\mathbf{k}.\mathbf{r}_2}] = \frac{1}{v} Y_2 \mathbf{w}. \tag{43}$$

Thus the polarization is attributed entirely to the displacement of the shell of the highly polarizable atom. In this regard, the displacement of the atoms **u** and the polarization which is decided by **w**, become independent quantities. In the rigid-ion model on the other hand, the polarization and the displacement of atoms are inherently related since it is the relative displacement of the atomic cores which causes a dipole moment to arise. So in the rigid-ion model which is devoid of shells, the approach of Askar *et al.*[13] will yield zero values for the polarization-gradient constants.

VI. RESULTS

In this section we present the values for the bulk flexoelectric constants for:

(i) *III-IV* semiconductors GaAs, GaP and II-VI semiconductor ZnS;

(ii) alkali halides NaCl and KCl;

and iii) perovskite dielectrics BTO and STO in their paraelectric phase.

Wherever possible we have tried to employ both *ab initio* and empirical shell-model lattice dynamics to estimate the values for the flexoelectric constants. However, in some cases only one of these techniques is used either due to lack of accurate shell-model potentials (for empirical lattice dynamics) or reliable pseudopotentials (for carrying out DFT based lattice dynamics). *Ab initio* phonon dispersions of GaAs were calculated in the local-density approximation (LDA) using a norm-conserving pseudopotential generated by Giannozzi *et al.*,[30] following a scheme proposed by von Barth and Car. A kinetic-energy cutoff of 25 Rydbergs (Ry) was chosen and 60**q** points were used for the Brillouin-zone (BZ) integration. An equilibrium lattice parameter of 5.612 Å as suggested by Giannozzi *et al.*[30] was chosen. The dynamical matrices were generated on an $8 \times 8 \times 8$ **k**-point mesh. *Ab initio* phonon dispersions of BTO were calculated in the LDA using Vanderbilt ultrasoft pseudopotentials. A

TABLE I. Flexoelectric constants for cubic semiconductors GaAs, GaP and ZnS from shell-model lattice dynamics

	μ_{11} (10^{-13} C/cm)		μ_{12} (10^{-13} C/cm)		μ_{44} (10^{-13} C/cm)	
	Ab initio	Shell model	*Ab initio*	Shell model	*Ab initio*	Shell model
GaAs	0.5144	0.8512	−0.8376	0.5107	0.2645	0.1702
GaP		0.4653		0.3128		−0.3443
ZnS		−0.311		−1.544		−0.611

kinetic-energy cutoff of 90 Ry was chosen and a Monkhorst $6\times6\times6$ grid of **q** points were used for the BZ integration. An equilibrium lattice parameter of 4.00 Å was used. The dynamical matrices were generated on an $8\times8\times8$ **k**-point mesh. *Ab initio* phonon dispersions of STO were calculated in the LDA using Vanderbilt ultrasoft pseudopotentials. A kinetic-energy cutoff of 90 Ry was chosen and a Monkhorst $6\times6\times6$ grid of **q** points were used for the BZ integration. An equilibrium lattice parameter of 3.85 Å was used. The dynamical matrices were generated on an $8\times8\times8$ **k**-point mesh. Parameters for the shell lattice-dynamical model for GaAs, GaP, and ZnS have been taken from Kunc *et al.*[31,32] Parameters for NaCl and KCl were taken from Askar *et al.*[13]

In order to find out the bulk flexoelectric constants the following methodology is used. From Eq. (20) it is clear that the flexoelectric constants can be related to the elements of the matrix **B** which in turn can be related to the real-space interatomic force constants as discussed in Sec. IV. Explicitly, these relations are given by Eq. (36b). First, the phonon-dispersion curves for the material under investigation are generated either by *ab initio* means (using Quantum ESPRESSO, a code which implements quantum-mechanical calculations using DFT) or/and empirical shell-model lattice dynamics. Then, in order to generate the matrix of interatomic force constants $\Phi^{nn'}_{ip,i'p'}$, an inverse Fourier transform is carried out on the dynamical matrix $C_{ip,i'p'}(\mathbf{k})$ [see Eq. (29)]. With this matrix of real-space interatomic force constants at hand, the methodology outlined in Sec. IV is used to generate the matrix **B** which can be related to the bulk flexoelectric tensor as given in Eq. (36b).

A. Semiconductors

For the case of the three semiconductors GaAs, GaP, and ZnS, no previous estimates for the flexoelectric constants exist. Our estimates for the flexoelectric constants are summarized in Table I.

The comparison of piezoelectric constants obtained from *ab initio* and shell-model lattice dynamics with experimental values is given in Table II.

B. Alkali halides

For the case of the NaCl and KCl, we have employed only empirical lattice dynamics to estimate the flexoelectric constants. Askar *et al.*[13] provided theoretical estimates using a single-ion polarizable shell model employing a different approach than ours. Our estimates using a similar model compare well with Askar *et al.*'s[13] estimates (Table III).

C. Perovskite dielectrics

For the case of the perovskite dielectrics STO and BTO we have employed only *ab initio* lattice dynamics to estimate the flexoelectric constants. Experimental estimates for the flexoelectric constants exist due to Zubko *et al.*[27] (for STO) and Ma and Cross[9] (for BTO) and they are compared with our estimates in Table IV. As one can see, our estimates for the flexoelectric constants of STO possess the same order of magnitude as those experimentally provided by Zubko *et al.*[27] On the other hand our estimate for μ_{12} of BTO is smaller than that estimated by Ma and Cross by *3 orders of magnitude*. It is interesting to note that in a recent *ab initio* study, scientists in Cambridge employed an alternative approach to estimate the flexoelectric constants of ferroelectric BTO and found them to be of the same order of magnitude as our estimates. The same group however report numbers close to Ma and Cross's[9] results for BTO while adopting an experimental approach. The possible reasons for such discrepancies are discussed in Sec. VII.

In a recent *ab initio* study, scientists at Cambridge[33] demonstrated, by employing an entirely different approach that the flexoelectric constants for perovskite dielectric BTO and Lead Titanate and paraelectric STO have flexoelectric constants in the range of 1 nC/m which, at least to an order of magnitude, agrees with our estimates.

VII. DISCUSSION AND SUMMARY

In light of the values obtained for the materials considered in the previous section, it is clear that flexoelectric constants

TABLE II. Piezoelectric constants for cubic semiconductors GaAs, GaP and ZnS obtained from shell-model lattice dynamics compared with existing experimental values.

	e_{14} (C/m^2)		
	Ab initio	Shell model	Experiment
GaAs	−0.1464	−0.066	−0.16
GaP		−0.0744	−0.1
ZnS		−0.111	−0.13

TABLE III. Flexoelectric constants for cubic alkali halides NaCl and KCl obtained by shell-model lattice dynamics compared with theoretical estimates by Askar *et al.* (Ref. 13).

	μ_{11} (10^{-13} C/cm)		μ_{12} (10^{-13} C/cm)		μ_{44} (10^{-13} C/cm)	
	Shell model	Askar *et al.*[a]	Shell model	Askar *et al.*[a]	Shell model	Askar *et al.*[a]
NaCl	0.412	0.423	−0.122	−0.119	−0.212	−0.230
KCl	0.403	0.411	−0.122	−0.120	−0.228	−0.231

[a]Reference 13.

of perovskite dielectrics like BTO, STO are larger than those of conventional dielectrics such as *III-IV* semiconductors, *II-VI* semiconductors and ionic salts such as NaCl by as much as *4* orders of magnitude. This peculiar property of incipient perovskite dielectrics can be attributed not only to their anomalously large born effective charges but also to the existence of strong coupling between the transverse-acoustic modes and the soft transverse optic modes so characteristic of incipient perovskite dielectrics.[34] This coupling lends itself to strong spatial dispersive effects which results in large atomic displacement responses to a nonhomogeneous mechanical stimulus. Consequently, the internal sublattice shifts for such perovskite dielectrics due to an applied strain gradient may be orders of magnitude higher than those exhibited by conventional dielectrics. The transverse-acoustic mode in such materials is known to exhibit anomalously large dispersion even at small k vectors, which suggest that elastic nonlocal effects in them may also be much larger than conventional materials.

As already indicated in the previous section, our estimates for STO are in the same order of magnitude as observed experimentally by Zubko *et al.*[27] A few important factors should be kept in mind while interpreting the results. Typically, experiments to measure flexoelectric constants employ finite-dimensional cantilever beams (for dynamic measurements) or thin films (subjected to static bending experiments). Due to the finite dimensions of these structures, surface polarization effects may affect the values of the measured flexoelectric constants. We report the bulk flexoelectric constants: surface flexoelectricity is omnipresent in experiments on finite structures [which the experiments employ] and does not disappear in the absence of a macroscopic electric field. There are indications though that surface flexoelectric constants may be several orders of magnitude lesser than bulk flexoelectric constants for high-permittivity materials and may not affect the values of the bulk flexoelectric constants measured in experiments. Further, broken symmetry at the surface of such finite structures may cause surface piezoelectricity which may contribute to the experimentally measured polarization. In addition as Zubko *et al.*[27] point out, recent works[35] have indicated surface regions which are 100 μms deep with local fluctuations of the ferroelastic phase transitions that may induce spontaneous flexoelectric polarization in addition to that resulting from inhomogeneous stress caused during bending experiments. In view of the above mentioned points, Zubko *et al.*[27] suggested that their measurements should be viewed as order-of-magnitude estimates. Considering the latter caveat, our results and those of Zubko *et al.* are in broad agreement. Further, from a theoretical point of view, the phonon dispersions from *ab initio* simulations are extremely sensitive to kinetic-energy cutoffs and the size of the grid employed to do Brillouin-zone integrations: the estimates of the unstable modes (which are important to capture the large flexoelectric constants of perovskite dielectrics) are therefore somewhat suspect though we have ensured that the interatomic force constants we use are sufficiently converged.

However, for the case of BTO, there is a large discrepancy between our estimates and the experimental results of Ma and Cross.[9] Another independent group of workers from Cambridge[33] have used both *ab initio* and experimental techniques to estimate the flexoelectric constants for BTO. It is interesting to note that while our estimates for BTO match those of their *ab initio* estimates, there exists a large discrepancy with their experimental results which are closer to those published by Ma and Cross.[9] The reason for this may be the extreme sensitivity of the soft optic mode to temperature in such perovskite dielectrics. At finite temperatures, at which experiments are performed, a large TA-TO coupling may exist which in turn can explain the rather high value of the

TABLE IV. Flexoelectric constants for cubic perovskite materials STO and BTO from *ab initio* calculations compared with available experimental data [Zubko *et al.* (Ref. 27) for STO and Ma and Cross (Ref. 9) for BTO].

	μ_{11} (10^{-13} C/cm)		μ_{12} (10^{-13} C/cm)		μ_{44} (10^{-13} C/cm)	
	Ab initio	Experiment	*Ab initio*	Experiment	*Ab initio*	Experiment
STO	−26.4	20	−374.7	700	−357.9	300
BTO	15.0		−546.3	10^6	−190.4	

flexoelectric constants consistently observed by Cross and co-workers[6–9] for several materials. Since our lattice dynamics calculations assume zero temperature, there is a possibility of the existence of such a large discrepancy.

The magnitude of the flexoelectric constants are known to scale as $f=\lambda\varepsilon e/a$, ε being the relative permittivity of the dielectric and λ being a dimensionless scaling factor. While from our results it is clear that the flexoelectric constants do scale with the dielectric constant: small flexoelectric constants are observed for conventional dielectrics with ε on the order of 10 and large flexoelectric constants are observed for perovskite dielectrics (3 to 4 orders of magnitude larger than conventional dielectrics) whose relative permittivity is of the order of 10^3, our results (as well as experiments by Zubko *et al.*[27]) suggest that the empirical scaling factor λ may be of the order of 10^{-2} which is in contrast to Ma and Cross[9] who estimate to $\lambda \sim 1$

ACKNOWLEDGMENTS

We acknowledge financial support from the NSF under NIRT Grants No. CMMI 0708096 and No. CMMI 0826153. Correspondence with G. Catalan is also gratefully appreciated. The second author benefited from discussions with A. Tagantsev during the writing of a review article.

*Corresponding author; psharma@uh.edu

[1] V. L. Indenbom, E. B. Loginov, and M. A. Osipov, Kristallografiya **26**, 1157 (1981).
[2] V. S. Mashkevich and K. B. Tolpygo, Sov. Phys. JETP **5**, 435 (1957).
[3] Sh. M. Kogan, Fiz. Tverd. Tela (Leningrad) **5**, 2829 (1963).
[4] A. K. Tagantsev, Phys. Rev. B **34**, 5883 (1986).
[5] A. K. Tagantsev, Phase Transitions **35**, 119 (1991).
[6] L. E. Cross, J. Mater. Sci. **41**, 53 (2006).
[7] W. Ma and L. E. Cross, Appl. Phys. Lett. **78**, 2920 (2001).
[8] W. Ma and L. E. Cross, Appl. Phys. Lett. **81**, 3440 (2002).
[9] W. Ma and L. E. Cross, Appl. Phys. Lett. **88**, 232902 (2006).
[10] R. D. Mindlin, Int. J. Solids Struct. **5**, 1197 (1969).
[11] L. D. Landau and E. M. Lifshitz, *Statistical Physics, Course of Theoretical Physics*, 3rd ed. (Butterworth-Heinemann, Oxford, 2000), Vol. 5.
[12] E. A. Eliseev, A. N. Morozovska, M. D. Glinchuk, and R. Blinc, Phys. Rev. B **79**, 165433 (2009).
[13] A. Askar, P. C. Y. Lee, and A. S. Cakmak, Phys. Rev. B **1**, 3525 (1970).
[14] R. Maranganti and P. Sharma, Phys. Rev. Lett. **98**, 195504 (2007).
[15] R. Maranganti and P. Sharma, J. Mech. Phys. Solids **55**, 1823 (2007).
[16] E. V. Bursian and N. N. Trunov, Fiz. Tverd. Tela (Leningrad) **16**, 1187 (1974).
[17] G. Catalan, L. J. Sinnamon, and J. M. Gregg, J. Phys.: Condens. Matter **16**, 2253 (2004).
[18] T. Dumitrica, C. M. Landis, and B. I. Yakobson, Chem. Phys. Lett. **360**, 182 (2002).
[19] S. M. Nakhmanson, A. Calzolari, V. Meunier, J. Bernholc, and M. Buongiorno Nardelli, Phys. Rev. B **67**, 235406 (2003).
[20] A. S. Nowick and W. R. Heller, Philos. Mag. **14**, 101 (1965).
[21] S. V. Kalinin and V. Meunier, Phys. Rev. B **77**, 033403 (2008).
[22] I. Naumov, A. M. Bratkovsky, and V. Ranjan, Phys. Rev. Lett. **102**, 217601 (2009).
[23] M. S. Majdoub, R. Maranganti, and P. Sharma, Phys. Rev. B **79**, 115412 (2009).
[24] M. S. Majdoub, P. Sharma, and T. Cagin, Phys. Rev. B **78**, 121407(R) (2008).
[25] M. S. Majdoub, P. Sharma, and T. Cagin, Phys. Rev. B **77**, 125424 (2008).
[26] N. D. Sharma, R. Maranganti, and P. Sharma, J. Mech. Phys. Solids **55**, 2328 (2007).
[27] P. Zubko, G. Catalan, P. R. L. Welche, A. Buckley, and J. F. Scott, Phys. Rev. Lett. **99**, 167601 (2007).
[28] E. Sahin and S. Dost, Int. J. Eng. Sci. **26**, 1231 (1988).
[29] M. Stengel and N. A. Spaldin, Nature (London) **443**, 679 (2006).
[30] P. Giannozzi, S. de Gironcoli, P. Pavone, and S. Baroni, Phys. Rev. B **43**, 7231 (1991).
[31] K. Kunc and O. H. Nielsen, Comput. Phys. Commun. **16**, 181 (1979).
[32] K. Kunc and O. H. Nielsen, Comput. Phys. Commun. **17**, 413 (1979).
[33] J. W. Hong, G. Catalan, J. F. Scott, and E. Artacho, private communication.
[34] J. D. Axe, J. Harada, and G. Shirane, Phys. Rev. B **1**, 1227 (1970).
[35] H. Hünnefeld, T. Niemöller, J. R. Schneider, U. Rütt, S. Rodewald, J. Fleig, and G. Shirane, Phys. Rev. B **66**, 014113 (2002).